Synthesis and Chemical Properties of Dielectric Polyphenylenes with Nitro Group

Masahiro Abe,[1] Masatoshi Tokita,[2] Junji Watanabe,[2] Yoshimasa Sakai,[3] Takakazu Yamamoto[1]

[1]*Chemical Resources Laboratory, Tokyo Institute of Technology, Midori-ku, Yokohama 226-8503, Japan*
[2]*Department of Organic and Polymeric Materials, Tokyo Institute of Technology, Ookayama, Meguro-ku, Tokyo 152-8552, Japan*
[3]*Mitsubishi Chemical Group Science and Technology Research Center, Inc., Aoba-ku, Yokohama 227-8502, Japan*

Received 17 June 2008; accepted 25 August 2008
DOI 10.1002/app.29287
Published online 21 November 2008 in Wiley InterScience (www.interscience.wiley.com).

ABSTRACT: Polyphenylenes consisting of nitrophenylene and didodecyloxy-*p*-phenylene units have been synthesized by Pd-catalyzed organometallic polycondensation. The polymers showed good solubility and had number–average molecular weights (M_n) of 13,000–37,000. Their spin-coated films showed fairly high dielectric constants (ε) of 3.75–6.36. The polymers were electrochemically active with electrochemical reduction peaks in the range of −1.72 to −1.99 V versus Ag^+/Ag in an acetonitrile solution of $[NEt_4]BF_4$ (0.10*M*). The polymer composed of 2,3′-dinitrobiphenyl and didodecyloxy-*p*-phenylene units showed thermotropic liquid crystalline phase at about 240°C. Cast films of the polymer had a birefringent phase at room temperature, suggesting self-assembly of the polymer in the solid. XRD studies revealed that the polymers assumed an ordered structure assisted by aggregation of the long alkoxy side chains in the solid. The polymer main chain in the cast film is considered to be aligned parallel with respect to the surface of substrates. © 2008 Wiley Periodicals, Inc. J Appl Polym Sci 111: 2426–2435, 2009

Key words: polyaromatics; liquid-crystalline polymers; orientation; polycondensation

INTRODUCTION

Poly(*p*-phenylene) (PPP) is one of the fundamental π-conjugated polymers, and various derivatives of PPP have been synthesized.[1–5] However, reports of PPP derivatives composed of electron-withdrawing nitro-*p*-phenylene units are limited.[6–9] Herein, we report the synthesis of new PPPs consisting of nitro-*p*-phenylene units such as

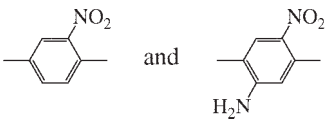

For the nitro-*p*-phenylene unit, poly(imide)s,[10–12] poly(arylester)s,[13–16] poly(arylene-vinylene)s,[17–19] and poly(aryleneethynylene)s[20,21] consisting of the unit have been reported, and polythiophenes[22–25] consisting of nitrothiophene have also been reported.

π-Conjugated polymers composed of 2,5-dialkoxy-*p*-phenylene units with long alkoxy side groups, e.g.,

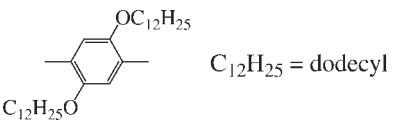

often show a strong tendency to self-assemble and to align on the surface of substrates.[26–28] Polyphenylenes consisting of nitro-*p*-phenylene and 2,5-dialkyoxy-*p*-phenylene units are also expected to self-assemble in an ordered structure, and this article reports the synthesis of new polyphenylenes composed of the two phenylene units.

Because they contain the polar nitrophenylene unit and the self-assembling 2,5-dialkoxy-*p*-phenylene unit,[9] the polymers obtained show interesting chemical and physical properties, such as a fairly large dielectric constant (ε = 3.75–6.36) and liquid crystalline behavior.

EXPERIMENTAL

Materials and general procedures

4,4′-Dibromobiphenyl, 2,5-bromonitrobenzene, 2,5-dibromoaniline, 2,6-dibromo-4-nitroaniline, and 2-isopropoxy-4,4,5,5-tetramethyl-1,3,2-dioxaborolane

Additional Supporting Information may be found in the online version of this article.

Correspondence to: T. Yamamoto (tyamamot@res.titech.ac.jp).

Contract grant sponsor: Ministry of Education, Culture, Sports, Science, and Technology, Japan.

were used as purchased. Solvents for the polymerization were distilled and stored under an inert gas (N_2 or Ar). Pd-catalyzed polymerization was carried out using standard Schlenk techniques. 4,4′-Dibromo-2,3′-dinitro-biphenyl,[29] 3,5-dibromonitrobenzene,[30] and 2,5-dibromo-4-nitroaniline[21] were prepared according to the literature. 1,4-Bis(4,4,5,5-tetramethyl-1,3,2-dioxa-borolan-2-yl)-2,5-bis(dodecyloxy)benzene (2) was prepared by the boronation of 1,4-dibromo-2,5-bis(dodecyloxy)benzene (1) with 2-isopropoxy-4,4,5,5-tetramethyl-1,3,2-dioxaborolane as described later.

1,4-Bis(4,4,5,5-tetramethyl-1,3,2-dioxaborolan-2-yl)-2,5-bis(dodecyloxy)benzene (2)

n-BuLi (4.2 mL of 2.5*M* solution in hexane, 10.5 mmol) was added dropwise to a solution of 1,4-dibromo-2,5-bis(decyloxy)benzene (2.5 g, 4.56 mmol) in THF (60 mL) at −78°C under argon. The solution was stirred at −78°C for 25 min, warmed to 0°C, and kept at 0°C for 15 min. The solution was cooled to −78°C again and the conditions were kept for 15 min. 2-Isopropoxy-4,4,5,5-tetramethyl-1,3,2-dioxaborolane (2.8 mL, 13.7 mmol) was added quickly. After the solution was warmed to room temperature and stirred over night, it was poured into water. The product was extracted with THF. The organic layer was washed with water and brine and dried over sodium sulfate. The solvent was removed by rotary evaporation. Recrystallization from hexane twice afforded **2** (50%) as a white solid. ^{1}H-NMR ($CDCl_3$, ppm): δ 7.08 (s, 2H), 3.94 (t, 4H), 1.84–1.23 (m, 64H), 0.88 (t, 6H). $^{13}C\{^1H\}$ NMR ($CDCl_3$, ppm): δ 157.61, 119.91, 83.42, 69.82, 31.97, 29.77, 29.76, 29.74, 29.70, 29.63, 29.40, 26.16, 24.93, 22.74, 14.17. FTIR (KBr, cm^{-1}): 2986, 2921, 2853, 1501, 1472, 1420, 1391, 1210, 1144, 1092, 1053, 965, 868, 776, 720. Anal. Calcd for $C_{42}H_{76}B_2O_6$: C, 72.20; H, 10.96; O, 13.74. Found: C, 72.30; H, 10.80; O, 13.97.

Polymerizations

The polymers were prepared by organometallic polycondensation using a Pd(0) complex, $Pd(PPh_3)_4$, as the catalyst. Details of the preparation of the polymers are described later.

P1

To a 50 mL Schlenk flask charged with 2,5-dibromonitrobenzene (281 mg, 1.0 mmol), **2** (699 mg, 1.0 mmol), and $Pd(PPh_3)_4$ (69 mg, 0.06 mmol), THF (15 mL) and 2*M* K_2CO_3 aq (15 mL) were added under nitrogen. The mixture was purged with nitrogen for 5 min and then stirred under reflux for 48 h. After cooling to room temperature, the solution was poured into methanol. The precipitate was separated by filtration and washed with H_2O and methanol. Reprecipitation of a chloroform solution of the polymer into methanol and drying under vacuum gave **P1** as a yellow solid (yield = 85%). ^{1}H-NMR ($CDCl_3$, ppm): δ 8.32 (br, 1H), 7.92 (br, 1H), 7.52 (br, 1H), 7.09 (d, 6.7 Hz, 1H), 6.97 (d, 6.1 Hz, 1H), 4.04 (br, 2H), 3.91 (br, 2H), 1.85–0.98 (m, 40H), 0.87 (br, 6H). FTIR (KBr, cm^{-1}): 2926, 2855, 1534, 1468, 1357, 1215, 1048. Anal. Calcd for $H(C_{36}H_{55}NO_4)_{38}Br$: C, 76.13; H, 9.77; N, 2.47; O, 11.27; Br, 0.37. M_n = 21582. Found: C, 75.50; H, 9.68; N, 2.50; O, 11.60; Br, 0.30. M_n = 21,000.

P2

The procedure was the same as for **P1**. Brown solid (yield = 88%). ^{1}H-NMR ($CDCl_3$, ppm): δ 8.34 (br, 1H), 8.20–7.95(m, 2H), 7.80–7.46 (m, 3H), 7.11 (s, 1H), 6.98(s, 1H), 4.08 (br, 2H), 3.93 (br, 2H), 1.91–0.99(m, 40H), 0.88 (br, 6H). FTIR (KBr, cm^{-1}): 2926, 2855, 1541, 1468, 1356, 1214, 1038. Anal. Calcd for $H(C_{42}H_{58}N_2O_6)_{44}Br$: C, 73.25; H, 8.49; N, 4.07; O, 13.94; Br, 0.26. M_n = 30,991. Found: C, 73.08; H, 8.63; N, 3.92; O, 14.22; Br, 0.20. M_n = 31,000.

P3

The procedure was the same as for **P1**. Yellow solid (yield = 88%). ^{1}H-NMR ($CDCl_3$, ppm): δ 8.05 (br, 1H), 7.04 (br, 1H), 6.91 (br, 1H), 6.97 (br, 1H), 4.45 (br, 2H), 3.98 (br, 2H), 3.88 (br, 2H), 1.90–0.78 (m, 46H). FTIR (KBr, cm^{-1}): 3492, 3388, 2927, 2854, 1625, 1508, 1390, 1322, 1258, 1210, 1037. Anal. Calcd for $H(C_{36}H_{56}N_2O_4)_{22}Br$: C, 73.97; H, 9.66; N, 4.79; O, 10.95; Br, 0.62. M_n = 12,859. Found: C, 73.47; H, 9.25; N, 4.65; O, 11.06; Br, 0.99. M_n = 13,000.

P4

The procedure was the same as for **P1**. Yellow solid (yield = 90%). ^{1}H-NMR ($CDCl_3$, ppm): δ 8.54 (br, 2H), 8.16 (br, 1H), 7.12 (br, 2H), 4.03 (br, 4H), 1.82–0.97 (m, 40H), 0.85(br, 6H). FTIR (KBr, cm^{-1}): 2926, 2854, 1535, 1509, 1459, 1346, 1213, 1037, 741. Anal. Calcd for $H(C_{36}H_{55}NO_4)_{66}Br$: C, 76.25; H, 9.78; N, 2.47; O, 11.29; Br, 0.21. M_n = 37,426. Found: C, 75.88; H, 9.94; N, 2.32; O, 11.68; Br, 0.10. M_n = 37,000.

P5

The procedure was the same as for **P1**. Yellow solid (yield = 80%). ^{1}H-NMR ($CDCl_3$, ppm): δ 8.15 (br, 2H), 7.03 (br, 2H), 4.63 (br, 2H), 4.00 (br, 4H), 1.90–0.75 (m, 40H), 0.85 (br, 6H). FTIR (KBr, cm^{-1}): 3501, 3399, 2928, 2854, 1617, 1499, 1469, 1383, 1326, 1212, 1107, 1033, 725. Anal. Calcd for $H(C_{36}H_{56}N_2O_4)_{33}Br$:

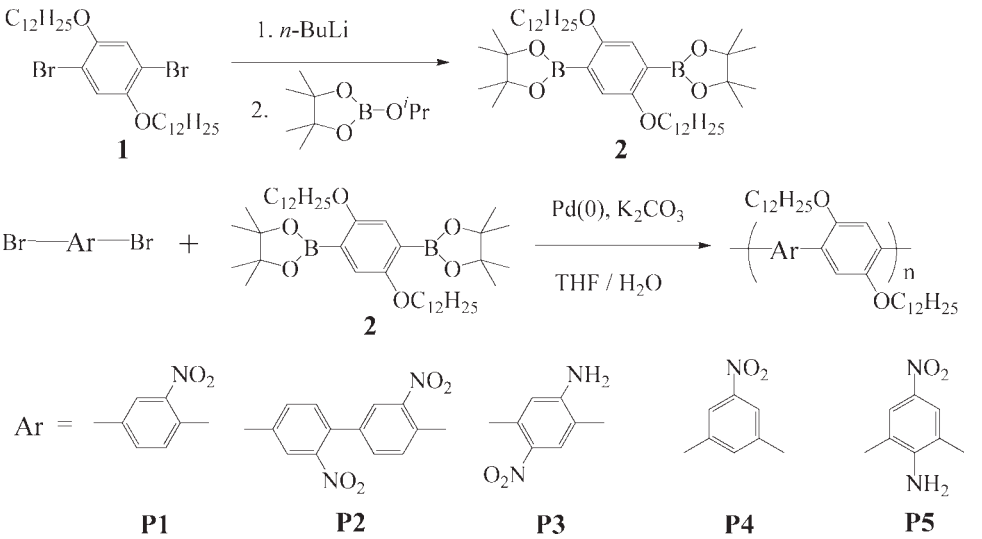

Scheme 1 Synthesis of nitro-polyphenylenes.

C, 74.13; H, 9.68; N, 4.80; O, 10.97; Br, 0.42. M_n = 19,249. Found: C, 73.70; H, 9.70; N, 4.58; O, 11.21; Br, 0.44. M_n = 19,000.

Measurements

NMR and IR spectra were recorded on a JEOL EX-400 spectrometer and JASCO FT/IR-460 Plus spectrometer, respectively. Elemental analysis was carried out with a LECO CHNS-932 analyzer and a Yanaco YS-10 SX-Elements microanalyzer. GPC traces were obtained with a Tosoh HLC-8120GPC chromatograph using chloroform as the eluent. Thermogravimetric analysis (TGA) and differential scanning calorimetry (DSC) were performed on Shimadzu TGA-50 and DSC-50 analyzers, respectively. UV–vis spectra were measured with a Shimadzu UV-3100 spectrometer. Cyclic voltammetry of cast films of the polymers on a Pt plate was performed in an acetonitrile solution containing $[Et_4N]BF_4$ (0.10*M*) under N_2 using a Pt counter electrode, an Ag^+/Ag reference electrode, and a Toyo Technica Solartron SI 1287 electron interface. Powder X-ray diffraction (XRD) patterns were recorded on a Rigaku RINT2100 diffractometer with a Cu Kα (1.54 Å) radiation. Density of polymers was measured by a sink and float method using aqueous solutions of $ZnCl_2$. The quantum chemical calculations were performed using Spartan'04. Ground-state geometries were optimized at the Becke's three-parameter hybrid functional using the Lee–Yang–Parr correlation functional (B3LYP)[31,32] level with the 6-31G* basis set.[33,34] Electrical conductivity was measured with a Custom CDM-5000E meter by a two probe method. Capacitance of the polymer was measured by Agilent precision LCR meter 4284A at 1 kHz. The thickness of spin-coating films of the polymer was determined by AFM (Nanopics NPX1000). The sandwich-type capacitor was fabricated as followed. A chloroform solution of the polymer (~ 3 wt %) was spin-coated on patterned ITO (indium tin oxide) glass. After spin-coating, the film was dried on a hot plate at 100°C for 1 h in a glovebox under N_2. A 200 nm Cr electrode was vapor-deposited. The capacitance between the electrodes was measured at 1 kHz. Using eq. (1), ε was calculated.

$$C = \varepsilon_0 \times \varepsilon \times S \times t^{-1} = 8.855 \times 10^{-12} \times \varepsilon \times S \times t^{-1} \quad (1)$$

where C is the capacitance (in F), S is the area of the film (in m^2), t is the thickness of the film (in m; cf. Fig. 8), ε_0 is the vacuum dielectric constant, and ε is the dielectric constant.

RESULTS AND DISCUSSION

Preparation of nitro-polyphenylenes

Scheme 1 shows synthetic routes to the monomers and polymers. **P1**, **P2**, and **P3**, consisting of

TABLE I
Results of Polymerization

Polymer	Yield (%)	M_n[a]	PDI[a,b]	DP[c]	T_d[d] (°C)
P1	85	2.1×10^4	2.1	37	340
P2	88	3.1×10^4	2.9	45	321
P3	88	1.3×10^4	1.8	22	327
P4	90	3.7×10^4	2.6	65	350
P5	80	1.9×10^4	1.8	32	325

[a] Estimated from GPC (eluent = chloroform, vs. polystyrene standards).
[b] Polydispersity index.
[c] Degree of polymerization calculated from M_n.
[d] 5% Weight-loss temperature measured by TGA under N_2, with a heating rate of 10°C min^{-1}.

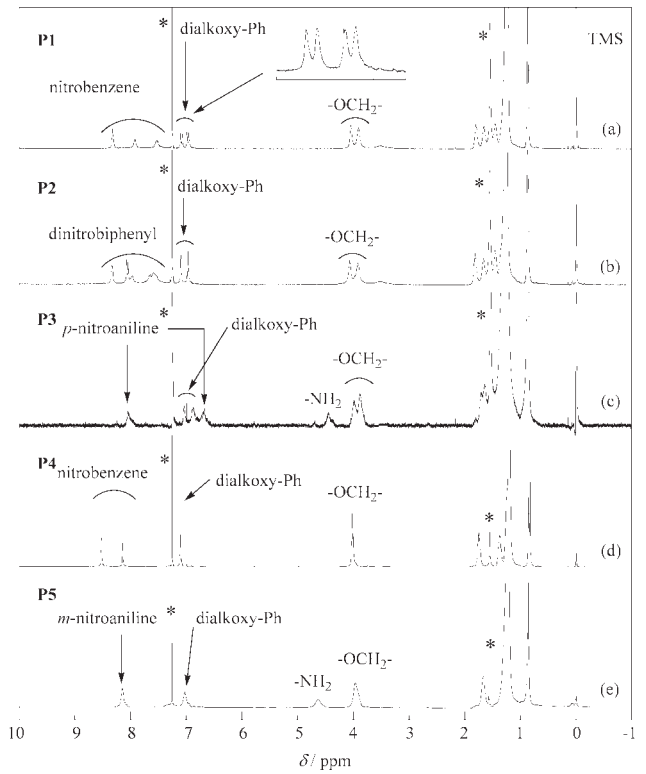

Figure 1 ^{1}H-NMR spectra (400 MHz) of (a) **P1**, (b) **P2**, (c) **P3**, (d) **P4**, and (e) **P5** in $CDCl_3$. The peaks with * are due to solvent impurities ($CHCl_3$ and H_2O).

alternating nitro-*p*-phenylene and 2,5-dodecyloxy-*p*-phenylene units, were synthesized via Suzuki-type polycondensation. For comparison, **P4** and **P5**, composed of 3-nitro-*m*-phenylene units, were also synthesized.

The polymerization results are summarized in Table I. Yields of the polymers were higher than 80%, and the number–average molecular weights, M_n, of the polymers estimated by GPC (versus polystyrene standards) ranged from 13,000 to 37,000. All the polymers were highly soluble in common organic solvents such as chloroform, THF, and toluene.

Figure 1 shows ^{1}H-NMR spectra of the polymers in $CDCl_3$. The area ratios between aromatic proton signals, aliphatic proton signals, and $-NH_2$ signal agree with the structures of the polymers.

P1 shows ^{1}H-NMR peaks at δ 8.32, 7.92, and 7.52 in a 1 : 1 : 1 area ratio, and they are assigned to aromatic protons of the *p*-nitrobenzene unit. All the polymers show aromatic proton peak(s) of the 2,5-di(dodecyloxy)-*p*-phenylene unit ($C_6H_2(OC_{12}H_{25})_2$-*p*) at about δ 7.1.

For **P1**, four aromatic proton peaks of the $C_6H_2(OC_{12}H_{25})_2$-*p* unit appear at δ 7.108, 7.073, 6.990, and 6.955, respectively, in about 1 : 1 : 1 : 1 ratio at 400 MHz (with separation of 14, 33, and 14 Hz). They are explained by the presence of the three triads, Triad-A through Triad-C, as described in Figure 2. Statistical distribution will give Triad-A, Triad-B, and Triad-C in a 1 : 2 : 1 ratio, which agrees with the appearance of the four peaks in the 1 : 1 : 1 : 1 ratio. These results suggest that the direction (or regioregularity) of the 3-nitro-*p*-phenylene unit is not controlled in **P1**. Appearance of only two sharp peaks at δ 7.108 and 6.979 for **P2** suggests control of the direction (or regioregularity) of the dinitrobiphenyl unit in a head-to-tail mode (cf. Fig. 2). However, it was difficult to obtain further evidence for a regiocontrolled polycondensation. It has been reported that such a regiocontrolled polycondensation could take place in some polycondensations assisted by side-chain aggregation (or crystallization).[35–37] **P4** and **P5** have a symmetrically nitrated *m*-phenylene unit, and they show a single aromatic proton peak for the 2,5-dodecyl-*p*-phenylene unit, as shown in Figure 1(d,e). **P3** and **P5** give rise to an NH_2 peak at about δ 4.5.

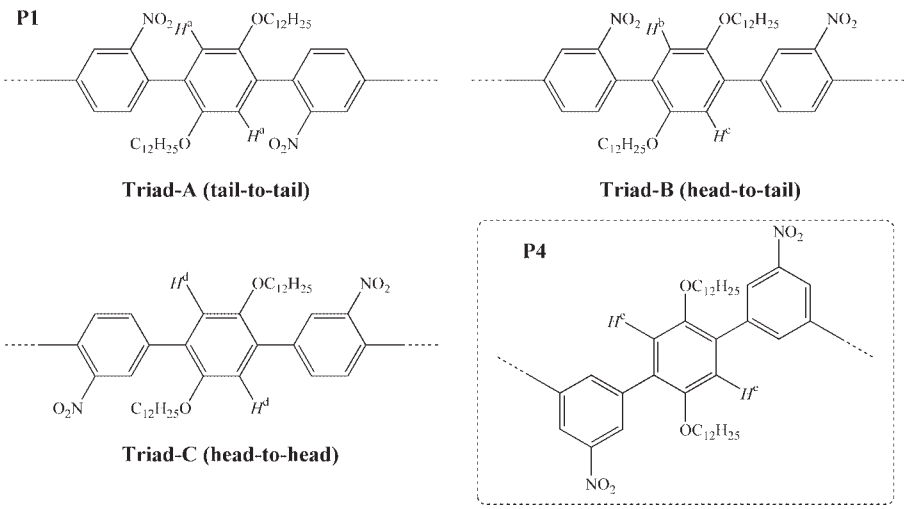

Figure 2 Possible triads in **P1** and **P4**.

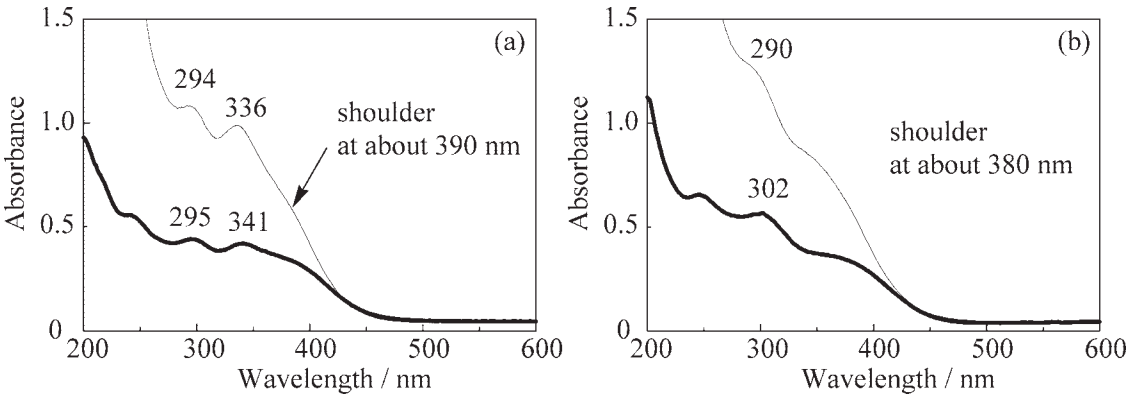

Figure 3 UV–vis spectra of (a) **P1** and (b) **P2** in chloroform (solid line) and in cast film (bold line).

IR spectra of the polymers were also reasonable for the molecular structures proposed. They show a characteristic $\nu_{asym}(NO_2)$ peak at about 1500 cm^{-1} and $\nu_{sym}(NO_2)$ peak at about 1350 cm^{-1} as exhibited in Figure S1 in Supporting Material. ν(N—H) peaks of **P3** and **P5** appeared in the range of 3300–3500 cm^{-1}, and δ(N—H) peaks of **P3** and **P5** were observed at 1625 and 1627 cm^{-1}, respectively.

TGA revealed that the polymers were thermally stable up to 300°C under N_2, and their 5% weight-loss temperatures (T_d) ranged from 321 to 350°C (cf. Table I and Fig. S2 in Supporting Material); the T_d values are comparable to that of a nitro-polyimide (T_d = 317°C).[10] Changes in the IR spectrum of **P2** after heating are shown in Figure S3.

Optical properties

Figure 3 shows UV–vis spectra of **P1** and **P2** in chloroform and in cast film. Optical and electrochemical data for the polymers are summarized in Table II. The main UV–vis peak position of **P1** in $CHCl_3$ (336 nm) is located near those of a copolymer of 1,4-phenylene and 2,5-dialkoxy-*p*-phenylene **3**[38,39] (∼ 340 nm) and a homopolymer of 2,5-dialkyoxy-*p*-phenylene[40] (∼ 340 nm).

TABLE II
Optical and Electrochemical Data of the Polymers

Polymer	λ_{max} in $CHCl_3$ (nm)	λ_{max} in film[a] (nm)	E_{ox}[b] (V)	E_{red}[b] (V)
P1	294, 336, ca. 390[c]	295, 341	1.12	−1.86
P2	290, 355[d], ca. 390[c]	302, 375[c]	1.08	−1.84
P3	280, 330, ca. 380[c]	281, 335	0.99	−1.99
P4	266, 332	269, 337	1.18	−1.72
P5	268, 332	268, 335	1.06, 1.24	−1.88

[a] Cast film on quartz plate.
[b] Electrochemical oxidation and reduction peak current potentials vs. Ag^+/Ag.
[c] Shoulder peak assigned to the CT band (cf. the text).
[d] Shoulder peak.

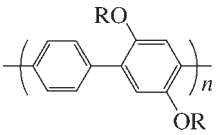

However, the UV–vis spectrum of **P1** seems to contain an absorption band at about 390 nm and the absorption edge of **P1** (∼ 450 nm) is observed at a longer wavelength compared with that of **3** (∼ 410 nm),[38,39] presumably because of the absorption band at about 390 nm. The absorption band at about 390 nm may be assigned to a charge transfer (CT) band (Scheme 2).

The shoulder peak at 390 nm obeyed Beer's low in a concentration range of 2.2×10^{-4}–1.4×10^{-5} M. As shown in Figure 3, the UV–vis absorption profile of **P1** in chloroform is essentially maintained in the cast film, indicating that electronic interaction caused by stacking[35–37,41–43] of the polymer molecules in the film is weak. The shoulder at about 390 nm becomes clearer in the cast film. **P2** shows an analogous UV–vis spectrum as shown in Figure 3(b). All the polymers showed no observable photoluminescence, which may be because of the quenching effect of nitro aromatic compounds.[44,45]

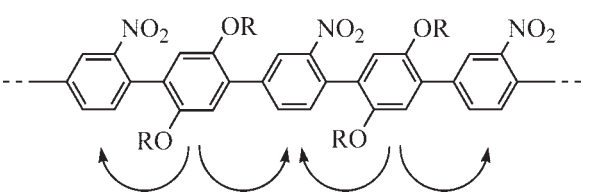

Scheme 2 Possible CT electron migration in photo-excitation.

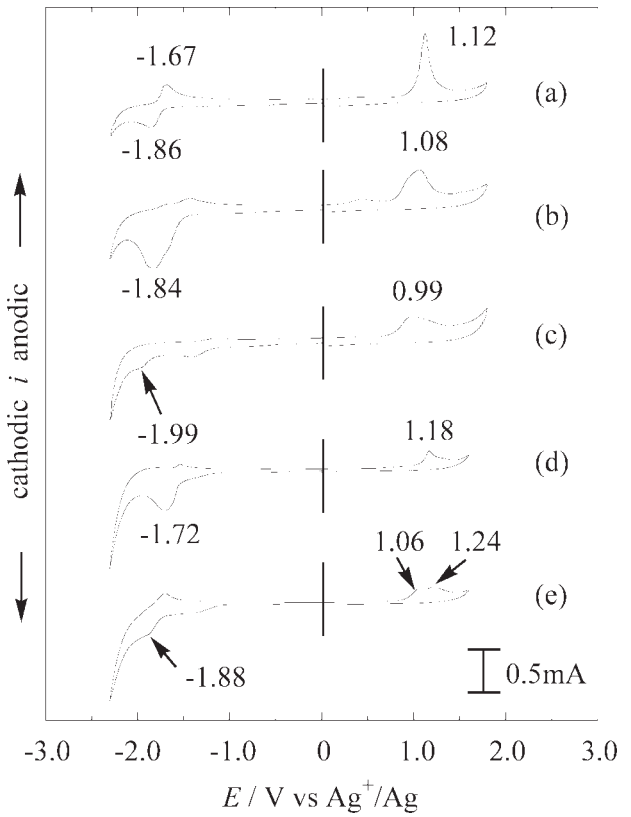

Figure 4 CV charts of (a) **P1**, (b) **P2**, (c) **P3**, (d) **P4**, and (e) **P5** films on a Pt plate in an acetonitrile solution of $[Et_4N]BF_4$ (0.10*M*) under N_2. The sweep rate is 50 mV s^{-1}.

Electrochemical response

Figure 4 shows cyclic voltammograms of cast films of **P1–P5** on a Pt plate in an acetonitrile solution of $[Et_4N]BF_4$ (0.10*M*) under N_2. Peak current electrochemical reduction (or *n*-doping) potentials (E_{pc}) of the polymers are observed in the range from −1.99 to −1.72 V versus Ag^+/Ag. The E_{pc} values are located as expected between those of PPP (E_{pc} = −2.6 V versus Ag^+/Ag)[46,47] and quantitatively nitrated PPP (NO_2/*p*-phenylene = about 1) (E_{pc} = −1.4 V versus Ag^+/Ag),[7] in view of the number density (1/2–2/3) of the NO_2 group per phenylene group. The CV charts show an *n*-dedoping peak at about −1.7 V versus Ag^+/Ag (e.g., −1.67 versus Ag^+/Ag for **P1**). For the data shown in Figure 4, scanning was started from 0 versus Ag^+/Ag in the cathodic direction; at −2.3 V versus Ag^+/Ag, a reverse scan to 1.7 V versus Ag^+/Ag was carried out. Scanning over a narrower range of 0 to −2.3 V versus Ag^+/Ag gave the cathodic peak in essentially the same position as that shown in Figure 4, and the CV curve was reproducible in the second scan when scanning was carried out between 0 and −2.3 V versus Ag^+/Ag. However, the *n*-doping and *n*-dedoping peaks became much weaker after one scan to the oxidation region between 0 and 1.7 versus Ag^+/Ag. Electrochemical *n*-doping of nitrated π-conjugated polymers has been reported.[48,49]

In the oxidation (or *p*-doping) region, all polymers give an irreversible oxidation peak at about 1.0 V versus Ag^+/Ag. Various π-conjugated polymers consisting of the 2,5-dialkoxy-*p*-phenylene units show such an irreversible *p*-doping peak,[27,50] and a strong trapping effect of the two alkoxy groups toward the anionic dopant (BF_4^- in this case) is proposed as an explanation. Once the polymer receives the irreversible *p*-doping, the electronic state of the polymer is changed and the *n*-doping and *n*-dedoping peaks are considered to be much weakened as described earlier.

Liquid crystalline behavior

As shown in Figure 5(a), **P2** displayed a birefringent liquid phase at 240°C, which is observed by polarized optical microscopy (POM). In DSC, the second heating and cooling curves of **P2** showed an endothermic peak at 233°C and an exothermic peak at 209°C, respectively, (Fig. S4 in Supporting

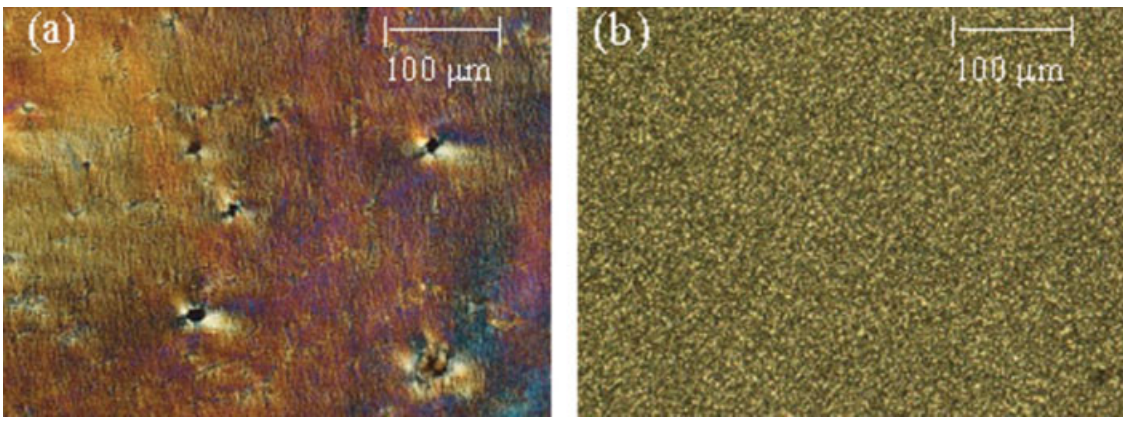

Figure 5 Polarized microscopic images of the polymers under crossed polarizers: (a) **P2** at 240°C and (b) **P3** in film at room temperature. [Color figure can be viewed in the online issue, which is available at www.interscience.wiley.com.]

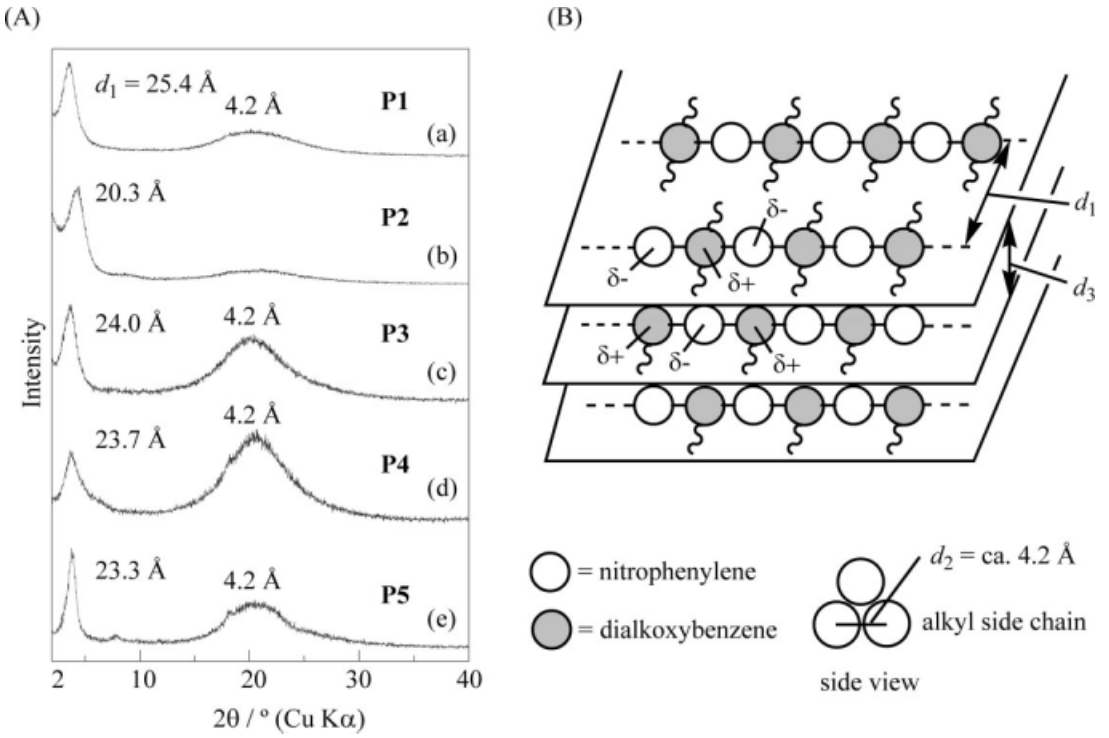

Figure 6 (A) Powder XRD patterns of (a) **P1**, (b) **P2**, (c) **P3**, (d) **P4**, and (e) **P5**. (B) Schematic packing structure of the polymer in the solid state.

Information). The endothermic peak at 233°C is attributed to crystal—LC phase transition. Connecting two points on the DSC curve where no thermal event takes place (e.g., 100 and 240°C) lets us know that the heating DSC curve includes a broad exothermic peak at 110–205°C and a small endothermic peak at 233°C. The broad exothermic peak can be attributed to melting of an unstable crystal followed by transformation to a stable one. The endothermic peak at 233°C is attributed to transformation of the stable crystal to the LC. The unstable crystal forms on cooling from the LC state because of kinetic reason. POM image measured at 240°C [Fig. 5(a)] is thus the optical texture of the LC phase.

These data indicate that **P2** behaves as a thermotropic liquid crystal. It has been reported that PPP derivatives having mesogenic cores in their side chains (e.g., **4**) have a nematic LC phase.[51,52]

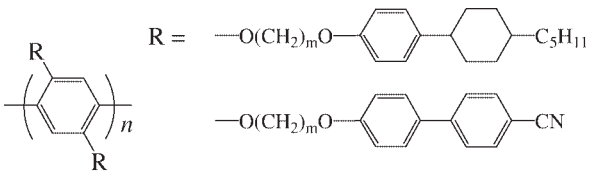

4

Liquid crystalline polyesters and poly(ester amide)s containing the nitrobenzene moiety in the main chain have also been reported.[14–16,53]

The polymers other than **P2** did not show such thermotropic LC behavior; however, they showed a birefringent phase in solution-cast films. Figure 5(b) shows a micrograph of a cast film of **P3** under the cross polarization conditions, which indicates the formation of an ordered aggregate in the solid state.

Powder X-ray diffraction

Figure 6(A) shows the powder XRD patterns of **P1**–**P5**. Various π-conjugated aromatic polymers with long alkyl or alkoxy side chains give an XRD peak in a low angle region ($2\theta < 5°$), and the peak has been attributed to the distance between the conjugated main chains separated by the alkyl or alkoxy side chains.[26–28,41–43] The XRD peaks with d_1 = 20.3–25.4 Å observed for **P1**–**P5** are also attributed to the distance between the main chains separated by the $OC_{12}H_{25}$ groups; the distance of 20.3–25.4 Å is reasonable for the thickness of the $C_6H_2(OC_{12}H_{25})_2$-*p* unit with tilted $OC_{12}H_{25}$ groups. Comb-like polymers having long alkyl side chains exhibit a reflection with a Bragg spacing of 4.2 Å, which is explained by pseudohexagonal packing of the alkyl side chains.[54,55] The broad XRD peak at 2θ = about 20° (or d_2 = 4.2 Å) suggests side chain aggregation. These results suggest that the polymers assume a layered packed structure because of the aggregation of long alkoxy side chains in the solid, as described in Figure 6(B).

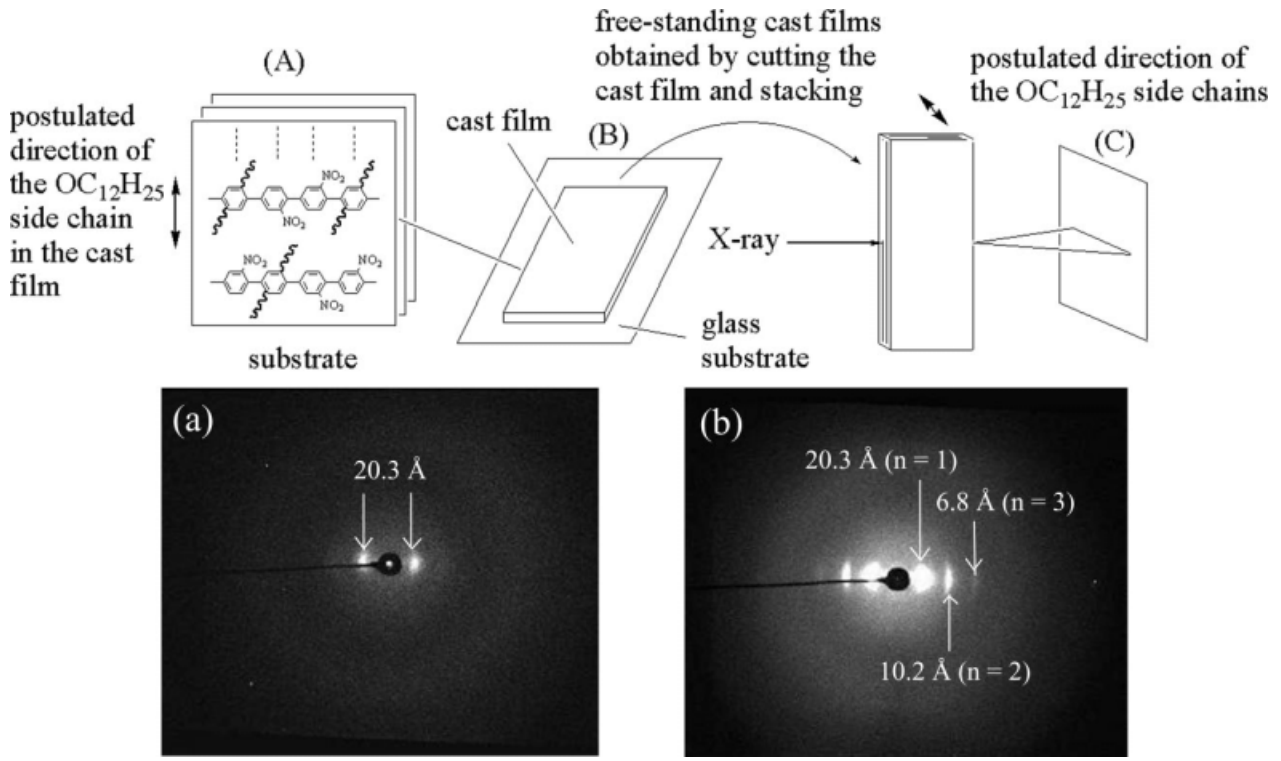

Figure 7 X-ray diffraction patterns measured for solution-cast film of **P2**: (a) as-prepared film at r.t; (b) after annealing at 200°C. The direction of the X-ray beam is shown in the drawing above the diffraction patterns.

The interlayer electronic interaction between negatively polarized nitrophenylene and positively polarized $C_6H_2(OC_{12}H_{25})_2$-*p* is thought to assist the formation of an ordered structure. However, the interlayer π-stacking, if it takes place, does not seem to be strong because of twisting of the main chain caused by the bulky NO_2 and $OC_{12}H_{25}$ groups; B3LYP/6-31G* level calculation for a model compound supports the twisting of the main chain (cf. Fig. S5). If the main chain is not twisted, the π-stacking distance is considered to be shorter than that (about 3.8 Å) observed for head-to-tail poly(3-alkylthiophene) because the polymers in this study do not contain a bulky S atom.[41] For the polymers consisting of C, O, and N, about 3.4 Å may be expected as the π-stacking distance.* A π-stacking distance of 3.4 Å gives calculated densities of 1.37, 1.38, and 1.48 g cm^{-3} for **P1**, **P2**, and **P3**, respectively.† The observed densities of 1.08, 1.03, 1.14, 1.29, and 1.28 for **P1**–**P5**, respectively, are considerably smaller than the calculated densities. This observation suggests that the polymers have longer interlayer distances [d_3 in Fig. 6(B)] of about 4.2 Å because of twisting of the main chain. This interpretation is consistent with the aforementioned optical data, which suggest a weak intermolecular electronic interaction in the solid state. That no XRD peak is observed at about $d = 3.4$ Å also supports this view.

X-ray diffraction of films

Cast films of **P1**–**P5** show XRD patterns similar to those of powdery samples (Fig. S6). However, the d_1 distances are somewhat different from those observed for the powdery samples, suggesting a different tilt angle of the $OC_{12}H_{25}$ group toward the main chain.

Two films of liquid crystalline **P2** were prepared on a quartz plate by solution-casting and spin-coating. Both films were annealed at 200°C for 1 h under N_2. The XRD pattern of the cast film before annealing gave a peak at 19.1 Å [Figs. S6(b) and S7(a)]. After annealing, the XRD peaks of the films became sharper [Fig. S7(a)], and the interchain distance d_1 became somewhat shorter. These data suggest that annealing the polymer brings about a highly ordered, closely packed structure. The spin-coated film also showed similar changes in XRD after annealing at 200°C. As shown in Figure S4, the thermal phase transition of **P2** starts at about 180°C. LC polymers

*Graphite and DNA have stacking distances of 3.25 and 3.4 Å, respectively.

†For example, the height of the repeating unit —$C_6H_3(NO_2)$—$C_6H_2(OC_{12}H_{25})$-*p* in **P1** is estimated to be about 8.0 Å. This height, the expected π-stacking distance (3.4 Å), the d_1 value (25.4 Å), and the molecular weight of the repeating unit in **P1** (566) give a calculated density of (566)/($8.0 \times 3.4 \times 25.4 \times 10^{-24} \times 6.0 \times 10^{23}$) = 1.37 g cm^{-3} for **P1**.

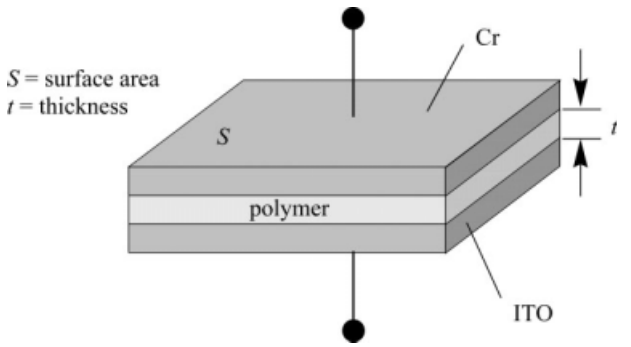

Figure 8 Schematic representation of sandwich-type capacitor. The cast film was sandwiched between the ITO and Cr electrodes.

often undergo a higher order alignment of polymer chains above the thermal phase transition temperature. In-plane XRD patterns of the cast and spin-coated films (Fig. S8) exhibit no d_1 peak suggesting that **P2** molecules are aligned on the surface of the glass substrate with the $OC_{12}H_{25}$ side chain oriented toward the surface of the substrate. Rigid π-conjugated polymers with long side chains such as $OC_{12}H_{25}$ often form an analogous aligned structure on the surface of substrates.[26–28]

To obtain more information about the solid structure of the cast film, a free-standing film prepared by solution-casting was analyzed by two-dimensional wide-angle X-ray diffraction (2D-WAXD). As shown in Figure 7(a), the 2D XRD pattern includes a pair of reflections on the equation line both at room temperature and at 200°C. The corresponding second- and third-order reflections were observed at 200°C. These data correspond to the alignment of **P2** on the surface of the substrate with the $OC_{12}H_{25}$ side chain oriented toward the surface of the substrate, which is depicted in the drawing above the diffraction patterns in Figure 7.

Dielectric constant

All the polymers behave almost as insulators and showed conductivities less than 10^{-8} S cm^{-1}. Using spin-coated films, dielectric constants of the polymers were estimated. Sandwich-type capacitors shown in Figure 8 were fabricated, and the dielectric constant was evaluated from the capacitance (C) of the capacitor. The polymers gave the following dielectric constants (ε).

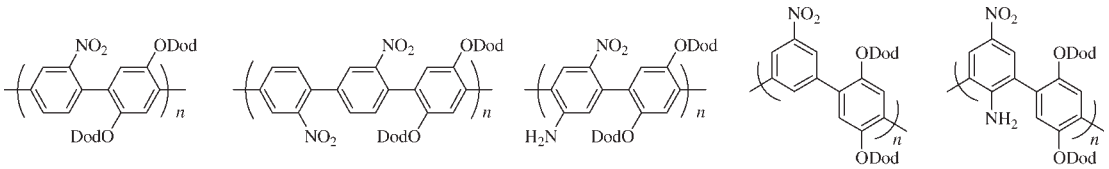

	P1	**P2**	**P3**	**P4**	**P5**
ε =	3.75	5.55	6.36	4.90	5.42

The dielectric constants are high and in the range of 3.75–6.36. **P3** and **P5** showed higher dielectric constant than **P1** and **P4**, because they contain the largely polarized *p*-nitroaniline unit. Inorganic dielectrics are used for organic field-effect transistors (OFET) as gate insulators (e.g., SiO_2 and Al_2O_3 show dielectric constants of 3.8[56] and 6–7,[57] respectively). Organic polymer gate dielectrics[58–62] such as poly(4-vinyl phenol) (ε = 3.9) and poly(vinyl alcohol) (ε = 8) are also employed. Because the nitrated polyphenylenes herein show good solution processability, good heat stability, and fairly high dielectric constants, they may find applications as gate dielectrics.

CONCLUSIONS

New polyphenylene derivatives having polar nitro groups and long alkoxy side chains have been synthesized. The polymers obtained are electrochemically active and have well-ordered structures as solids and high dielectric constants.

The authors are grateful to Mr. S. Aramaki of Mitsubishi Chemical Group Science and Technology Research Center, Inc. for helpful discussion.

References

1. Skotheim, T. A.; Elsenbaumer, R. L.; Reynolds, J. R., Eds. Handbook of Conducting Polymers, 2nd ed.; Dekker: New York, 1997.
2. Skotheim, T. A.; Reynolds, J. R., Eds. Handbook of Conducting Polymers, 3rd ed.; CRC Press: Boca Raton, FL, 2007.
3. Nalwa, H. S., Ed. Handbook of Organic Conductive Materials and Polymers; Wiley: Chichester, U. K., 1997.
4. Yamamoto, T.; Koizumi, T. Polymer 2007, 48, 5449.
5. Schlüter, A. D. J Polym Sci Part A: Polym Chem 2001, 39, 1533.

6. Kowitz, C.; Wegner, G. Tetrahedron 1997, 53, 15553.
7. Yamamoto, T.; Abe, M.; Wu, B.; Choi, B.-K.; Harada, Y.; Takahashi, Y.; Kawata, K.; Sasaki, S.; Kubota, K. Macromolecules 2007, 40, 5504.
8. Wirth, H. O.; Müller, R.; Kern, W. Makromol Chem 1964, 77, 90.
9. Abe, M.; Tokita, M.; Watanabe, J.; Sakai, Y; Yamamoto, T. Polym Prepr, Jpn 2006, 55, 2627.
10. Qiu, Z.; Chen, G.; Zhang, Q.; Zhang, S. Eur Polym J 2007, 43, 194.
11. Wang, H.-H.; Wu, S.-P. J Appl Polym Sci 2004, 93, 2072.
12. Wang, H.-H.; Wu, S.-P. J Polym Res 2005, 12, 37.
13. Jin, J.-I.; Choi, E.-J.; Jo, B.-W. Macromolecules 1987, 20, 934.
14. Lin, J.; Sherrington, D. C.; Nield, E.; Richards, R. W. Macromolecules 1992, 25, 7107.
15. Takahashi, H.; Horie, K.; Yamashita, T.; Machida, S.; Hannah, D. T. B.; Sherrington, D. C. Macromol Chem Phys 1996, 197, 2703.
16. Sato, M.; Uemoto, Y. Macromol Rapid Commun 2000, 21, 1220.
17. Pan, M.; Bao, Z.; Yu, L. Macromolecules 1995, 28, 5151.
18. Koßmehl, G.; Samandari, M. Makromol Chem 1985, 186, 1565.
19. Jin, J.-I.; Yu, S.-H.; Shim, H.-K. J Polym Sci Part B: Polym Phys 1993, 31, 87.
20. Moroni, M.; Le Moigne, J.; Luzzati, S. Macromolecules 1994, 27, 562.
21. Koishi, K.; Ikeda, T.; Kondo, K.; Sakaguchi, T.; Kamada, K.; Tawa, K.; Ohta, K. Macromol Chem Phys 2000, 201, 525.
22. Yamamoto, T.; Yamada, W.; Takagi, M.; Kizu, K.; Maruyama, T.; Ooba, N.; Tomaru, S.; Kurihara, T.; Kaino, T.; Kubota, K. Macromolecules 1994, 27, 6620.
23. Zhang, Q. T.; Tour, J. M. J Am Chem Soc 1998, 120, 5355.
24. Li, Y.; Vamvounis, G.; Holdcroft, S. Macromolecules 2001, 34, 141.
25. Li, Y.; Vamvounis, G.; Holdcroft, S. Macromolecules 2002, 35, 6900.
26. Yamamoto, T.; Kokubo, H.; Morikita, T. J Polym Sci Part B: Polym Phys 2001, 39, 1713.
27. Yamamoto, T.; Fang, Q.; Morikita, T. Macromolecules 2003, 36, 4262.
28. Yamamoto, T.; Ootsuka, H.; Iijima, T. Macromol Rapid Commun 2007, 28, 1786.
29. Maya, F.; Tour, J. M. Tetrahedron 2004, 60, 81.
30. Chanteau, S. H.; Tour, J. M. J Org Chem 2003, 68, 8050.
31. Becke, A. D. J Chem Phys 1993, 98, 5648.
32. Lee, C.; Yang, W.; Parr, R. Phys Rev B 1988, 37, 785.
33. Hariharan, P. C.; Pople, J. A. Chem Phys Lett 1972, 16, 217.
34. Hariharan, P. C.; Pople, J. A. Theor Chim Acta 1973, 28, 213.
35. Yamamoto, T.; Arai, M.; Kokubo, H.; Sasaki, S. Macromolecules 2003, 36, 7986.
36. Yamamoto, T.; Arai, M.; Kokubo, H.; Sasaki, S. J Polym Sci Part A: Polym Chem 2003, 41, 1449.
37. Yamamoto, T.; Kokubo, H.; Kobashi, M.; Sakai, Y. Chem Mater 2004, 16, 4616.
38. Shin, S.-H.; Park, J.-S.; Park, J.-W.; Kim, H. K. Synth Met 1999, 102, 1060.
39. Harrison, B. S.; Ramey, M. B.; Reynolds, J. R.; Schanze, K. S. J Am Chem Soc 2000, 122, 8561.
40. Vahlenkamp, T.; Wegner, G. Macromol Chem Phys 1994, 195, 1933.
41. McCullough, R. D.; Tristam-Nagle, S.; Williams, S. P.; Sowe, R. D.; Jayaraman, M. J Am Chem Soc 1993, 115, 4910.
42. Morikita, T.; Yamaguchi, I.; Yamamoto, T. Adv Mater 2001, 13, 1862.
43. Chen, T.-A.; Wu, X.; Rieke, R. D. J Am Chem Soc 1995, 117, 233.
44. Yang, J.-S.; Swager, T. M. J Am Chem Soc 1998, 120, 5321.
45. Yang, J.-S.; Swager, T. M. J Am Chem Soc 1998, 120, 11864.
46. Fauvarque, J.-F.; Petit, M.-A.; Digua, A.; Froyer, G. Makromol Chem 1987, 188, 1833.
47. Rault-Berthelot, J.; Tahri-Hassani, J. J Electroanal Chem 1996, 408, 247.
48. Zhang, Q.; Li, Y.; Yang, M. Synth Met 2004, 146, 69.
49. Choi, B.-K.; Takahashi, H.; Kanbara, T.; Yamamoto, T. Polym J 2000, 32, 991.
50. Shiraishi, K.; Yamamoto, T. Synth Met 2002, 130, 139.
51. Oguma, J.; Akagi, K.; Shirakawa, H. Synth Met 1999, 101, 86.
52. Oguma, J.; Kawamoto, R.; Goto, H.; Itoh, K.; Akagi, K. Synth Met 2001, 119, 537.
53. Sandhya, K. Y.; Pillai, C. K. S.; Kumar, K. S. J Polym Sci Part B: Polym Phys 2004, 42, 1289.
54. Jordan, E. F., Jr.; Felderisen, D. W.; Wrigley, A. N. J Polym Sci Part A-1: Polym Chem 1971, 9, 1835.
55. Hsieh, H. W. S.; Post, B.; Morawetz, H. J Polym Sci Polym Phys Ed 1976, 14, 1241.
56. Fuoss, R. M. J Am Chem Soc 1937, 59, 1703.
57. Zhou, W.; Qi, S.; Tu, C.; Zhao, H.; Wang, C.; Kou, J. J Appl Polym Sci 2007, 104, 1312.
58. Wang, L.; Yoon, M.-H.; Facchetti, A.; Marks, T. J Adv Mater 2007, 19, 3252.
59. Kim, C.; Facchetti, A.; Marks, T. J. Science 2007, 318, 76.
60. Sun, Y.; Liu, Y.; Ma, Y.; Di, C.; Wang, Y.; Wu, W.; Yu, G.; Hu, W.; Zhu, D. Appl Phys Lett 2006, 88, 242113.
61. Singh, T. B.; Meghdadi, S.; Günes, S.; Marjanovic, N.; Horowitz, G.; Lang, P.; Bauer, S.; Sariciftci, N. S. Adv Mater 2005, 17, 2315.
62. Schroeder, R.; Majewski, L. A.; Grell, M. Adv Mater 2005, 17, 1535.